

## Figure S1. Mitochondrial dysfunction promotes xenobiotic response. Related to Figure 1.

- (A) Genes involved in detoxification and immunity are induced by *spg-7* RNAi (Nargund et al., 2012).
- (B) Model of mitochondrial surveillance and xenobiotic response.
- (C) Animals were collected similar to those photographed in (Figure 1A) for western blot.
- (D) Quantification of fluorescent intensities of animals shown in (Figure 1B); \*\*\*\*  $p < 0.0001$ .
- (E) Animals were collected similar to those photographed in (Figure 1B) for western blot.
- (F-K) Animals carrying *cyp-14A4p::gfp* animals were challenged by *P. aeruginosa* (F and G), tunicamycin, hydrogen peroxide (H and I), and heat shock (J and K). Animals were photographed in (F, H and J), and the fluorescent intensities were quantified in (G, I and K). Scale bars, 100  $\mu$ m. \*  $p < 0.05$ , \*\*\*\*  $p < 0.0001$ ; ns, not significant.
- (L and M) *cyp-14A4p::gfp* animals feeding on control RNAi or RNAi of the subunits of mitochondrial electron transport chain at 20°C. Animals were photographed in (L), and the fluorescent intensities were quantified in (M). Scale bar, 100  $\mu$ m. \*\*\*\*  $p < 0.0001$ .
- (N and O) *cyp-14A4p::gfp* animals feeding on control RNAi or RNAi of designated mitochondrial or other essential genes at 20°C. Animals were photographed in (N), and collected for western blot in (O). Scale bar, 100  $\mu$ m.
- (P) Strategy of genetic screen seeking mutants that activate *cyp-14A4p::gfp*.
- (Q and R) Location and identities of *hsp-6* mutations used in the study.
- (S) BLAST of *C. elegans* HSP-6 to other HSP70 family proteins.
- (T) Quantification of fluorescent intensities of animals shown in (Figure 1C), \*\*\*\*  $p < 0.0001$ .
- (U) Animals were collected from samples similar to those shown in (Figure 1C) for western blot.
- (V and W) Synchronized L1 larvae of wild-type and *hsp-6*(mg585) animals were grown at 20°C or 25°C. 2 days post L1 animals are shown in (V). Scale bar, 200  $\mu$ m. Animals at each stage were counted in (W).
- (X) The brood size of wild-type and *hsp-6*(mg585) animals.
- (Y and Z) Comparison of the upregulated genes from *hsp-6*(mg585) mRNA-seq with previous *spg-7* RNAi microarray by Venn diagram and volcano analysis in (Y); and with previous *hsp-6* RNAi microarray by Venn diagram and volcano analysis in (Z).

*nduf-7*: mitochondrial complex I NADH dehydrogenase; *sdhb-1*: mitochondrial complex II succinate dehydrogenase; *cyc-1*: mitochondrial complex III cytochrome reductase; *cco-1*: mitochondrial complex IV cytochrome oxidase; *asp-1*: mitochondrial complex V ATP synthase; *atp-4*: mitochondrial complex V ATP synthase; *timm-23*: mitochondrial inner membrane translocase; *tomm-40*: mitochondrial outer membrane translocase; *tba-2*: alpha-tubulin; *dhc-1*: dynein heavy chain; *act-1*: actin; *unc-60*: actin depolymerizing factor/cofilin; *pbs-2*: proteasome beta subunit; *rpn-1*: 26S proteasome regulatory subunit; *rps-12*: ribosomal small subunit; *rpl-27*: ribosomal large subunit; *hsp-4*: Hsp70/grp78/BiP; *sec-24.2*: COPII SEC24B.





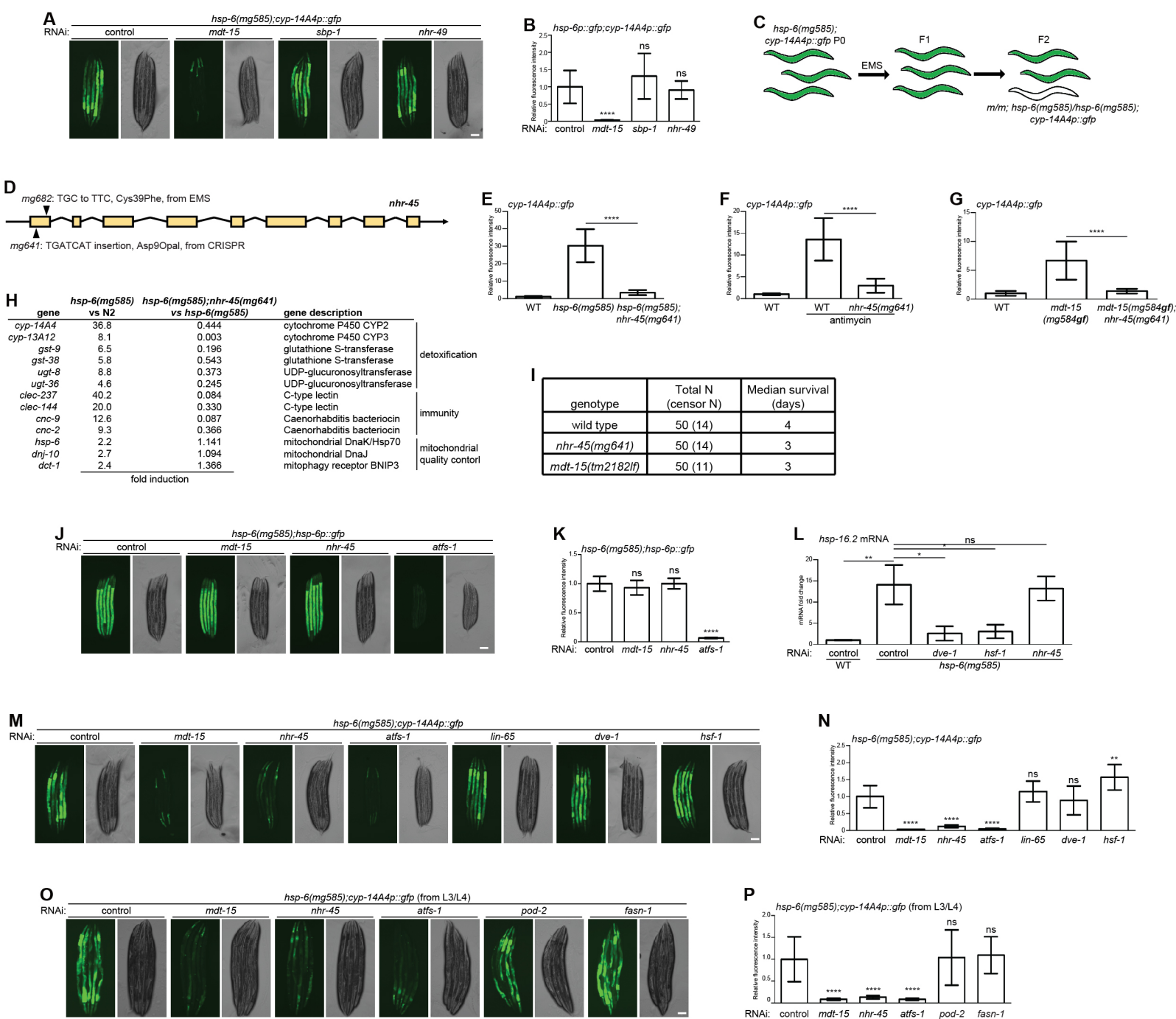


**Figure S3. MDT-15 and NHR-45 regulate xenobiotic responses to mitochondrial dysfunction. Related to Figure 3.**

(A and B) Synchronized L1 larvae of *hsp-6(mg585);cyp-14A4p::gfp* animals were grown with control RNAi or RNAi of indicated genes at 20°C for three days. Animals were photographed in (A), and the fluorescent intensities were quantified in (B). Scale bar, 100 μm.

(C) Strategy of genetic screen seeking mutants that abolished the activation of *cyp-14A4p::gfp* in *hsp-6(mg585)* genetic background.

(D) Information of *nhr-45* mutants.

(E-G) Quantification of fluorescent intensities of animals shown in (Figure 3A-3C); \*\*\*\*  $p < 0.0001$ .

(H) Representative genes that are regulated by *nhr-45*.

(I) Survival analysis of wild-type, *mdt-15(tm2182lf)*, and *nhr-45(mg641)* on *P. aeruginosa* PA14 strain.

(J and K) Synchronized L1 larvae of *hsp-6(mg585);hsp-6p::gfp* animals were grown with control RNAi or RNAi of indicated genes at 20°C for three days. Animals were photographed in (J), and the fluorescent intensities were quantified in (K). Scale bar, 100 μm. \*\*\*\*  $p < 0.0001$ ; ns, not significant.

(L) Synchronized L1 larvae of wild-type and *hsp-6(mg585)* animals were grown with control RNAi or RNAi of indicated genes at 20°C for two days until L4 larval stage. Animals were collected and analyzed by RT-qPCR toward *hsp-16.2* with *act-1* as control. \*  $p < 0.05$ ; \*\*  $p < 0.01$ ; ns, not significant.

(M and N) Synchronized L1 larvae of *hsp-6(mg585);cyp-14A4p::gfp* animals were grown with control RNAi or RNAi of indicated genes at 20°C for three days. Animals were photographed in (M), and the fluorescent intensities were quantified in (N). Scale bar, 100 μm. \*\*  $p < 0.01$ ; \*\*\*\*  $p < 0.0001$ ; ns, not significant.

(O and P) Synchronized L1 larvae of *hsp-6(mg585);cyp-14A4p::gfp* animals were grown 20°C for two days until L3/L4 larval stage and then transferred to control RNAi or RNAi of indicated genes at 20°C for another three days. Animals were photographed in (O), and the fluorescent intensities were quantified in (P). Scale bar, 100 μm. \*\*\*\*  $p < 0.0001$ ; ns, not significant.

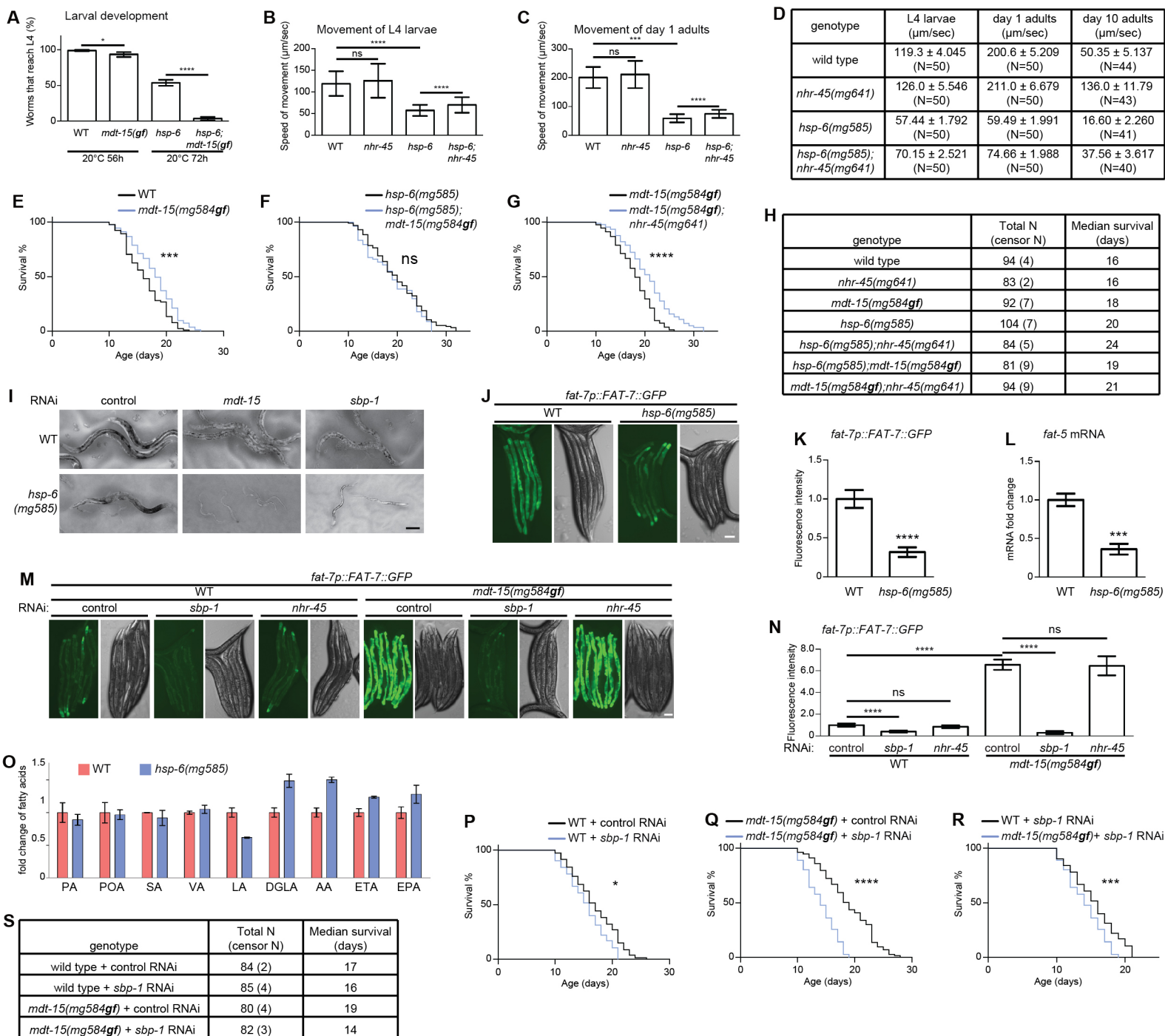


**Figure S4. Dissection of detoxification response and fat metabolism in *mdt-15(mg584gf)* mutant. Related to Figure 4.**

(A) Egg laying was performed to adult animals of indicated genetic background at 20°C for 1 h. After removal of the mothers, eggs were grown at 20°C for 56 h or 72 h. Worms that reach L4 larval stage were counted. \*  $p < 0.05$ ; \*\*\*\*  $p < 0.0001$ .

(B-D) The movements of L4 larvae (B) and day 1 adults (C) of indicated genetic background were estimated, and the detailed information was listed in (D). \*\*\*  $p < 0.001$ ; \*\*\*\*  $p < 0.0001$ ; ns, not significant.

(E-H) Life span analysis of animals of indicated genetic background. \*\*\*  $p < 0.001$ ; \*\*\*\*  $p < 0.0001$ ; ns, not significant.

(I) Synchronized L1 larvae of wild-type and *hsp-6(mg585)* animals were grown with control RNAi, *mdt-15* RNAi, or *sbp-1* RNAi at 25°C for 56 h or 80 h. Scale bar, 100 µm.

(J and K) Day 1 adult of wild-type and *hsp-6(mg585)* animals harboring *nls590[fat-7::fat-7::GFP]* transgene were photographed (J) and fluorescent intensities were quantified (K). Scale bar, 100 µm. \*\*\*\*  $p < 0.0001$ .

(L) L4 larvae of wild-type and *hsp-6(mg585)* animals were analyzed by RT-qPCR toward *fat-5* with *act-1* as control. \*\*\*  $p < 0.001$ .

(M and N) Synchronized L1 larvae of wild-type and *mdt-15(mg584gf)* animals harboring *nls590[fat-7::fat-7::GFP]* transgene were treated with control RNAi or RNAi of *sbp-1* or *nhr-45* at 20°C for 3 days. The worms were photographed (M) and fluorescent intensities were quantified (N). Scale bar, 100 µm. \*\*\*\*  $p < 0.0001$ ; ns, not significant.

(O) Fatty acids analysis of wild-type and *hsp-6(mg585)* L4 stage animals by gas chromatography. PA: palmitic acid; POA: palmitoleic acid; SA: stearic acid; VA: vaccenic acid; LA: linoleic acid; DGLA: dihomo- $\gamma$ -linolenic acid; AA: arachidonic acid; ETA: eicosatetraenoic acid; EPA: eicosapentaenoic acid.

(P-S) Life span analysis of wild-type and *mdt-15(mg584gf)* animals with control RNAi or *sbp-1* RNAi. \*  $p < 0.05$ ; \*\*\*\*  $p < 0.0001$ .



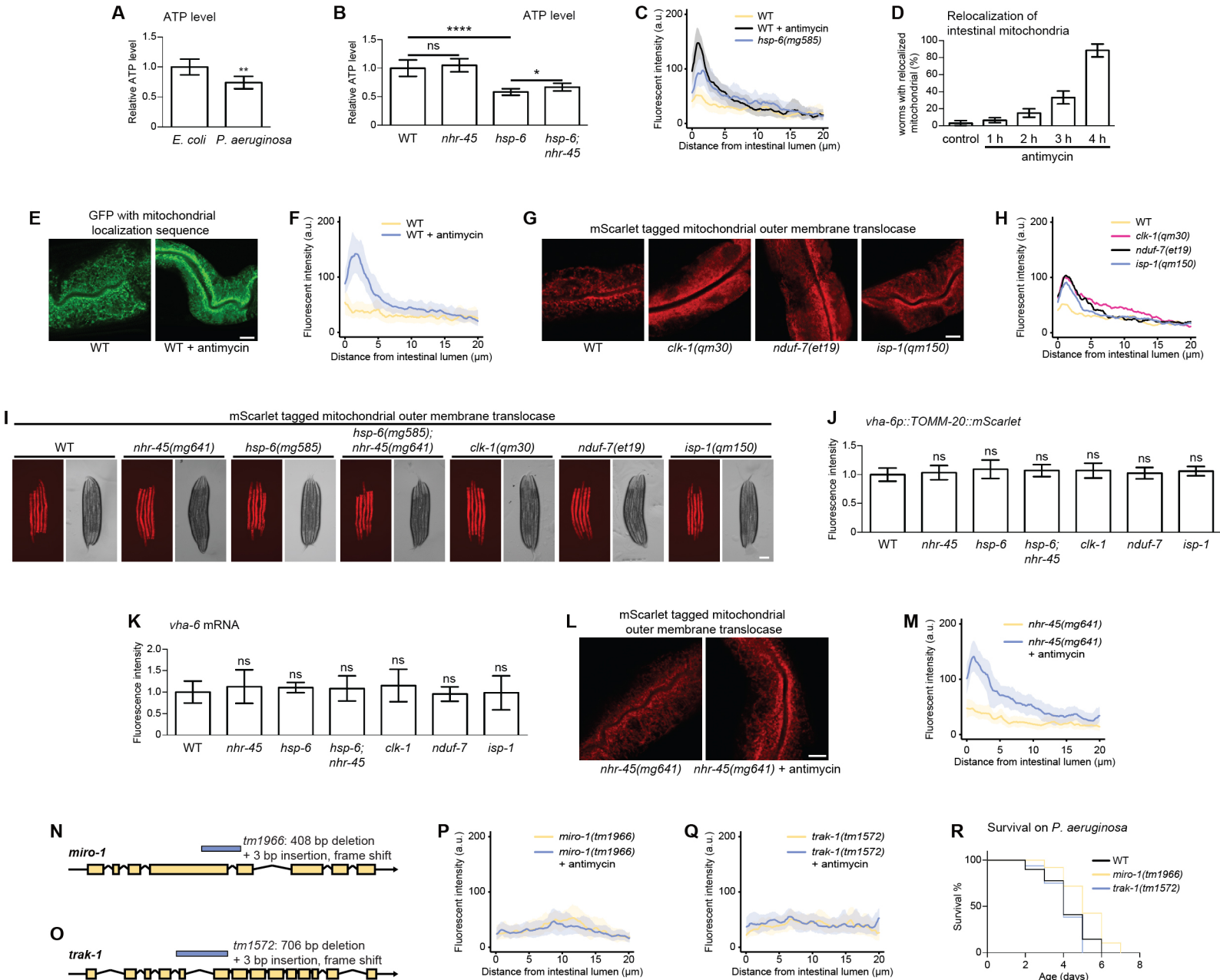


**Figure S5. Mitochondrial dysfunction causes the redistribution of mitochondria in intestinal cells. Related to Figure 5.**

(A) Synchronized wild-type L1 larvae were grown on *E. coli* OP50 or *P. aeruginosa* PA14 at 25°C until L4 larval stage. Worms were collected for determination of ATP level. \*\*  $p < 0.01$ .

(B) L4 larvae of indicated genetic background were collected for determination of ATP level. \*  $p < 0.05$ ; \*\*\*\*  $p < 0.0001$ ; ns, not significant.

(C) The fluorescent intensities of animals shown in (Figure 5B) was analyzed. The shading area indicates standard error.

(D) Wild-type L4 larvae were treated with antimycin, and the percentage of worms with relocated intestinal mitochondria was calculated.

(E-H) Animals of indicated genetic background with *zcls17[ges-1p::GFP(mit)]* in (E and F), and *mgTi33[vha-6p::tomm-20(1-54)::mScarlet]* transgene in (G and H) were grown with or without antimycin. Day one adults were photographed in (E and G). Scale bars, 10  $\mu\text{m}$ . The fluorescent intensity was analyzed by Fiji-ImageJ, and five different lines were drawn in each animal from three individuals in (F and H). The shaded area indicates standard error in (F), and was hidden in (H) for display of the data clearly.

(I and J) L4 larvae with indicated genetic background were pictured in (I), and the fluorescent intensities were quantified in (J). ns, not significant.

(K) L4 larvae of indicated genetic background were collected and analyzed by RT-qPCR toward *vha-6* with *act-1* as control. ns, not significant.

(L and M) Day one adults of *nhr-45(mg641)* animals with *mgTi33[vha-6p::tomm-20(1-54)::mScarlet]* transgene were photographed. Antimycin treatment was performed at L4 larvae. Scale bars, 10  $\mu\text{m}$ .

(N and O) Information of *miro-1* and *trak-1* mutants.

(P and Q) The fluorescent intensities of (Figure 5C) were analyzed. The shading area indicates standard error.

(R) Survival analysis of wild-type, *miro-1(tm1966)*, and *trak-1(tm1572)* animals on *P. aeruginosa* PA14 strain.